

Dynamic Modelling of a Hybrid Variable Reluctance Machine Using the 3D Finite Element Method

Dingamadji Hilaire Belembara¹, Jérôme Mbaïnaïbeye²

¹Department of Physics and Engineering Sciences, University of N'Djamena, N'Djamena, Chad

²Department of Physics, University of Moundou, Moundou, Chad

Email: hbelembara@gmail.com

How to cite this paper: Belembara, D.H. and Mbaïnaïbeye, J. (2024) Dynamic Modelling of a Hybrid Variable Reluctance Machine Using the 3D Finite Element Method. *Journal of Electromagnetic Analysis and Applications*, **16**, 103-113.

<https://doi.org/10.4236/jemaa.2024.167007>

Received: May 19, 2024

Accepted: July 28, 2024

Published: July 31, 2024

Copyright © 2024 by author(s) and Scientific Research Publishing Inc.

This work is licensed under the Creative Commons Attribution International License (CC BY 4.0).

<http://creativecommons.org/licenses/by/4.0/>



Open Access

Abstract

This paper presents the work carried out to evaluate the dynamic performance of the Hybrid Variable Reluctance Motor (HVRM). The fourth-order Runge-Kutta integration algorithm was employed to solve the equations of the dynamic model, in conjunction with the three-dimensional finite element method. The 3D numerical data was calculated using Comsol Multiphysics, which accounts for the nonlinearity of the ferromagnetic material and the 3D nature of the HVRM. The outcomes of this study are precise and accurately predict the dynamic behaviour of the HVRM in terms of rotor position response, rotational speed and torque. The distinctive contribution of this work lies in the 3D numerical modelling of the HVRM and the subsequent evaluation and analysis of its dynamic operation. Analytical and numerical 2D studies are less resource-intensive and time-consuming, and are more straightforward and rapid to analyse and interpret. However, they are constrained in their capacity to examine spatial, volumetric interactions and intricate dynamics such as flux studies where three 3D effects cannot be disregarded, winding end effects and the configuration and positioning of the interposed permanent magnet.

Keywords

Numerical Computing, Complex Dynamic, Flux Linkage, 3D Effects, Equilibrium Position

1. Introduction

Hybrid stepper motors are most often used in drive systems where positioning and holding are required. These types of machines, which were previously less at-

tractive due to torque ripples, are now experiencing an unexpected resurgence [1]. This renewed interest is due to their torque density, which is linked to the use of rare-Earth materials, as well as their high resolution compared with other types of motors. A number of research projects have been conducted with the objective of reducing or eliminating torque ripples through the implementation of various techniques and strategic controls [2]-[6].

In particular, the four-phase hybrid stepper motor represents an optimal solution for systems requiring high torque at low speed and high positional accuracy in comparison to two- or three-phase motors.

The accurate prediction of the characteristics of hybrid stepper motors is a significant concern for researchers and manufacturers alike. It is evident that the technique of accounting for their structural characteristics and non-linearity remains a crucial step in the analysis and optimisation of their parameters.

A coupled analytical two-dimensional finite element method for the study and optimisation of hybrid stepper machine parameters, utilizing the numerical simulation software outlined in [7], has been developed. However, this study does not consider the axial components of the physical quantities associated with the equivalent magnetic circuit.

The equivalent magnetic circuit method was developed and applied to the analysis of stepper motors in [8]. Although this method is flexible and does not require a significant amount of storage space, it is not sufficiently accurate.

In [8] and [9], the authors posit that the 3D Finite Element Method (MEF) represents a superior numerical simulation option, offering more accurate results. This is because the results of 3D finite element analysis take into account the non-linear characteristics, the small air gap of the motor and its three-dimensional nature.

The objective of this paper is to present a three-dimensional dynamic study of the four-phase hybrid stepper machine. Prior to this study, a three-dimensional finite element analysis was conducted to calculate the magnetic field. Furthermore, this method considers the localised saturation of the ferromagnetic material and the complex geometry of the rotor/stator teeth. Consequently, the outcomes of the three-dimensional finite element analysis are integrated into the dynamic model of the hybrid stepper motor in order to evaluate its dynamic performance. The assessment of the performance of an electric machine represents a pivotal stage in the design process. The objective is to optimise the energy efficiency, reliability and durability of the machine. A comprehensive performance evaluation serves to guarantee the correct operation of a specific application. By understanding and measuring the performance of the machine according to defined criteria and taking into account its intended use, it is possible to ensure that the machine meets the needs and requirements of the end user. Furthermore, this process enables any issues or constraints to be identified and rectified, thereby optimising the machine's performance. The dynamic electrical and mechanical models coupled to MEF 3D are solved as a matrix of state quantities, including position, rotational speed, torque, and other quantities of the machine's equivalent magnetic circuit.

The aforementioned state quantities are evaluated by considering two distinct types of tests, namely the no-load test and the load test. The specific test to be employed is dependent upon the value of the regulated electrical current, I , and the residual magnetism, B_r .

The remainder of the paper is organised as follows: Section 2 presents a description of a dynamic system with its different variables, the definition of the electrical and mechanical parameters of a variable reluctance machine, and the dynamics of a hybrid variable reluctance machine; the modelling results are presented in Section 3; finally, Section 4 presents the conclusion and perspectives of this work.

2. Materials and Methods

2.1. Materials

The two armatures are constructed from soft iron, which exhibits no magnetic losses. The hybrid variable reluctance machine under investigation comprises two half-machines, which are assumed to be homopolar and just matched through a permanent magnet. The permanent magnet utilised is based on rare Earth, specifically neodymium-iron-boron. The rotor is composed of two half-rings, which are offset mechanically by half an electrical period. The machine under consideration (**Figure 1** is an exploded version of **Figure 2**) is a double salient hybrid variable reluctance motor. The rotor has 50 evenly spaced teeth, while the stator has 8 studs, each with 5 teeth. **Figure 3** illustrates the outcome of the three-dimensional finite element analysis, which serves as the foundation for the dynamic model.

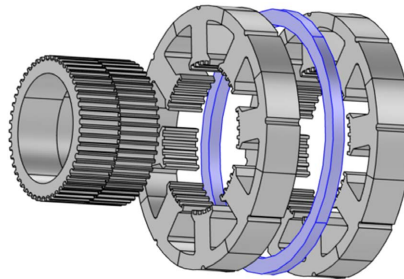


Figure 1. Exploded 3D geometry of the HVRM.

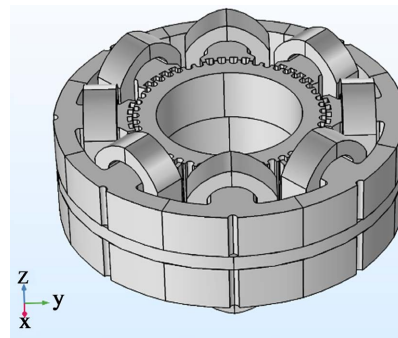


Figure 2. 3D geometry of the HVRM.

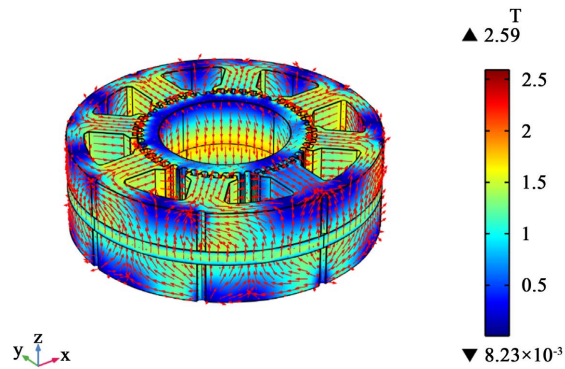


Figure 3. Magnetic map of the HVRM.

2.2. Methods

The fundamental principle of this method is the calculation of the phase fluxes utilising the three-dimensional finite element method. Subsequently, the results of the numerical calculation are integrated into the dynamic model in order to account for the non-linearity and local saturation of the ferromagnetic material.

2.2.1. Description of a Dynamic System

A dynamic system can be defined as a process that evolves over time. From an observer's point of view, a process corresponds to a physical system considered in the context of the evaluation of exchanges with its environment [10].

Various variables can be identified in a process:

- Control inputs, which are the external physical quantities whose variation contributes to the evolution of the system's behaviour;
- Disturbance inputs, which are generally uncontrollable by the user and which also act on the process;
- State variables, internal variables of the system, whose action on the environment is not necessarily directly perceptible but whose evolution governs that of the process.

The study of physical processes generally aims to:

- Understand how the system works and predict its behaviour and performance in the face of variations in inputs; this is known as system analysis;
- Seek to control the system's output and performance by acting on the inputs; In this case, it is a matter of synthesising control laws.

In order to analyse or synthesise control laws, it is often necessary to establish a model of the processes being studied. The process of modelling is primarily concerned with the construction of a mathematical description of the behaviour of the physical system [10]-[14]. This description is based on the fundamental principles of mathematics and is expressed in a language that is accessible to both humans and computers. There are two main types of model: knowledge models and representation and control models. It is crucial to acknowledge that the model is typically a mere abstraction of the phenomenon under investigation.

In the context of our study, the state model is the most suitable for the analysis of dynamic behaviour. This model represents a relationship between the state va-

riables $x(t)$, which constitute the memory of the system, and the control input variables $u(t)$. This model is typically represented by a system of ordinary differential equations relating to the state, together with an observation equation. In this instance, the dynamic system can be defined by the following equation of state:

$$\begin{cases} \dot{x}(t) = f(x, t, u) \\ x(0) = x_0 \end{cases} \quad (1)$$

The system output is given by Equation (2):

$$y(t) = g(x, u) \quad (2)$$

x : The state vector of components $x_i(\cdot)$, $\forall i = 1, 2, \dots, n$, $u \in R^n$;

t : The time, $t \in R_+$;

u : The command vector, with components $u_j(\cdot)$, $\forall j = 1, 2, \dots, m$, $x \in R^m$;

y : The output vector, components $y_i(\cdot)$, $\forall i = 1, 2, \dots, l$, $x \in R^l$;

\dot{x} : The derivative with respect to time of the state vector x ;

$f(\cdot)$: A vector function with components $f_i(\cdot)$, $\forall i = 1, 2, \dots, n$;

$g(\cdot)$: A vector function with components $g_k(\cdot)$, $\forall k = 1, 2, \dots, l$.

Non-linearities in the model are expressed in terms of the $f(\cdot)$ and $g(\cdot)$ functions.

The focus of this study is on complex continuous-time dynamic systems, as variable reluctance machines present complex and highly non-linear dynamic models, particularly when certain inherent phenomena in their operation are taken into account.

A dynamic system is described as complex to express the difficulty of either describing it properly or studying some of its functional aspects. This difficulty is generally due to the system's structure, which refers to the form of the relationships between its various parts or attributes [10] [15]-[17].

2.2.2. Definition of Electrical and Mechanical Parameters

Table 1 shows electrical and mechanical parameters employed during the no-load and load tests.

Table 1. Type electrical and mechanical parameters.

Designation	Symbol	Value
Resistance per phase	R	33 Ω
Moment of inertia of the machine	J	$3 \cdot 10^{-6}$ kg·m ²
Power supply control frequency	f	10 Hz
Current reference to be set	I_{ref}	0.55 A
Reverse voltage of zener diodes	V_z	3 V
DC bus voltage	U	60 V
Load torque	Γ_L	0.0045 N·m
Viscous friction coefficient	f_v	0.006 N·m/rad/s

2.2.3. Dynamics of a Hybrid Variable Reluctance Machine

In a hybrid variable reluctance machine, the state variables undergo changes in response to various parameters, including the position of the rotor and the currents in the windings. Over time, these variables can fluctuate in response to operating conditions and control commands, as well as due to the permanent magnet. As the machine operates, the position of the rotor can influence the distribution of magnetic flux, which in turn affects the electromagnetic characteristics of the machine. Furthermore, the currents in the windings may fluctuate in accordance with the load requirements and the control frequency, which also affects the machine's performance. It is of interest to ascertain the dynamic model of this machine. By means of a simulation of the model, it is possible to predict the machine's behaviour over time in accordance with specific operating conditions. The order of supply of the phases is as follows: The sequence of supply is as follows: 4-3-2-1.

1) Electrical dynamics

The electrical dynamics of an HVRM are characterised by its ability to respond when voltages are applied across the coils to generate a magnetic field and move the rotor precisely, although this compromises speed and torque. Upon the application of a voltage U across the coil of a phase of an HVRM, an electric current is created within the coil. This current generates a magnetic field that interacts with the permanent magnet to produce electromagnetic torque, which in turn causes the rotor to move. This phenomenon is governed by Equation (3):

$$U = Ri + \frac{d\Psi}{dt} \quad (3)$$

U : Applied voltage;

i : Current in the coil;

R : Phase resistance;

ψ : Phase magnetic flux. Given that the phenomenon of saturation of the magnetic circuit is considered, the phase magnetic flux is a non-linear function of the electric current and the rotor position, and can therefore be written as $\psi(\theta, i)$. Consequently, Equation (3) can be expressed as a partial differential equation (Equation (4)):

$$U = Ri + \frac{\partial\Psi(\theta, i)}{\partial i} \frac{di}{dt} + \frac{\partial\Psi(\theta, i)}{\partial \theta} \frac{d\theta}{dt} \quad (4)$$

Assuming that the four phases of the machine are identical, the generalised electrical dynamics for a phase j can be expressed by Equation (5):

$$\frac{di_j}{dt} = + \left(\frac{\partial\Psi(\theta, i_j)}{\partial i_j} \right)^{-1} \left(U_j + Ri_j - \frac{\partial\Psi(\theta, i_j)}{\partial \theta} \frac{d\theta}{dt} \right) \quad (5)$$

$\frac{\partial\Psi(\theta, i_j)}{\partial i_j}$: Represents the incremental inductance, which is a measure of the variation of the inductance of a coil as a function of the position of the rotor;

$\frac{\partial \Psi(\theta, i_j)}{\partial \theta}$: Represents the back electromotive force per unit speed or back electromotive voltage per unit speed.

2) Mechanical dynamics

The mechanical dynamics of an HVVRM can be modelled by the equations of rotor position (Equation (6)) and speed (Equation (7)). This model enables the understanding of the reaction of the system (machine) to the forces and torques applied to it, as well as to external load conditions. An understanding of these dynamics allows for the prediction of the machine's behaviour and the envisaging of precise control as a function of the situation.

$$\frac{d\theta}{dt} = \Omega \quad (6)$$

$$\frac{d\Omega}{dt} = \frac{1}{J} [T_e(\theta, i) - C_r - f_v \Omega] \quad (7)$$

C_r : Load torque;

f_v : Coefficient of viscous friction;

J : Moment of inertia;

T_e : Total electromagnetic torque (sum of the torque produced by the three phases).

3. Results and Discussions

Figure 4 illustrates the temporal evolution of the current in phase 4, wherein all phases exhibit identical characteristics. The figure demonstrates that the current curves in a phase are superimposable when the machine is running at no load ($C_r = 0 \text{ N}\cdot\text{m}$) or at load ($C_r = 0.0045 \text{ N}\cdot\text{m}$). From this figure, it can be concluded that no additional adjustments are required to the power supply device in order to drive a predefined load.

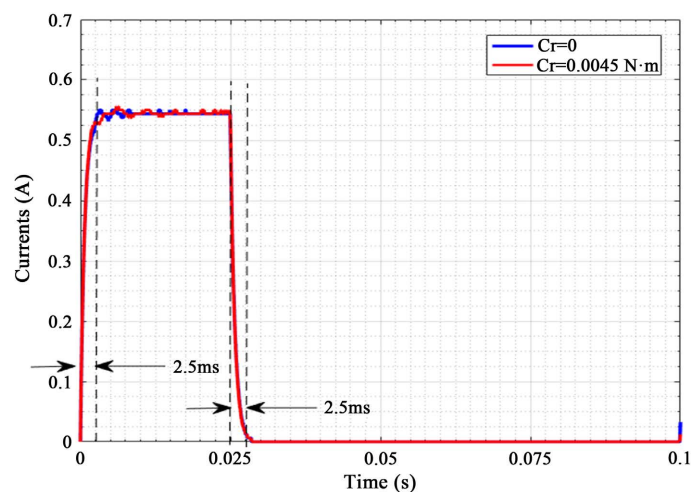


Figure 4. Evolution of currents in the phases.

Upon initial startup, the phase currents exhibit a rapid increase in amplitude

for a period $\Delta t_1 = 0.25$ ms before reaching a stable equilibrium value (0.55 A) for the remainder of the supply period of a phase. Subsequently, the phase currents decrease for a period $\Delta t_2 = 0.25$ ms before cancelling out. It can be concluded that, regardless of whether the machine is operating at no load or under load, a current of 0.55 A is drawn in order to provide the torque required on the output shaft to drive a load of 0.0045 N·m. Furthermore, it can be demonstrated that the current in one phase only cancels out when the current in the next phase reaches its maximum value ($\Delta t_1 = \Delta t_2$).

Figure 5 presents a comparison of the rotor positions during the elementary step-by-step movements between the no-load and loaded tests. The figure illustrates that there is a discrepancy in angular position between the elementary steps at no load and at load, with a difference of approximately 0.0075 rad. It is evident that the reduction in the elementary pitch under load is a consequence of the intensity of the load to be driven. However, the position response time for the loaded machine is greater than that for the unloaded machine. It is observed that at no load, the position response is quasi-stable at 5 ms before the commencement of a new step, whereas there are minor fluctuations that persist until the conclusion of the step for the machine under load.

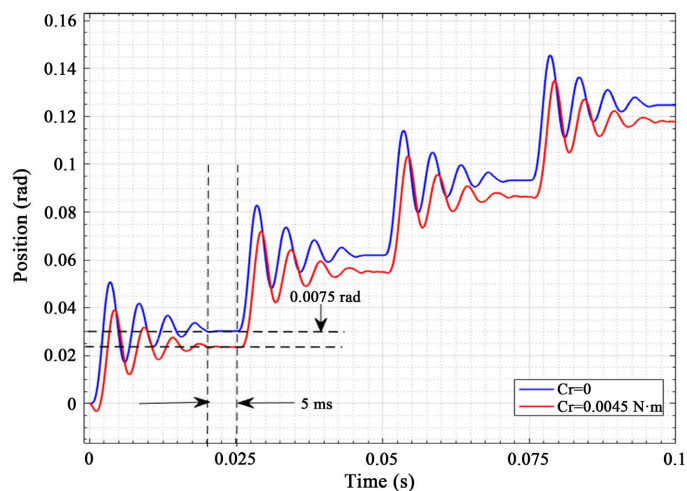


Figure 5. Rotor positions under load and at no load.

Figure 6 presents a comparison of the rotational speeds. **Figure 6** illustrates that the reduction in the elementary step of rotor displacement, as depicted in **Figure 4**, exerts an influence on the speed for the same test. In fact, the speed of rotation for the machine under load is reduced in comparison to that of the machine running at no load. It can be observed that the speed of the machine operating without a load stabilises before the conclusion of the control period, whereas the fluctuations only subside when the machine is in motion and driving a load.

Figure 7 presents a comparison of the electromagnetic torques developed by the machine during the no-load and load tests. From this figure, it can be ob-

served that the average torque at no load is zero, which is in accordance with Equation (6). Given that the machine is supplied with direct current, it can be demonstrated that the torque is inversely proportional to the speed of rotation. Consequently, the torque displayed in **Figure 7** increases during the load test, thereby corroborating the fact that the speed has decreased during the same test, as evidenced by the results presented in **Figure 6**. It can be stated that the average torque supplied to the output shaft of this machine under load, as shown in **Figure 7**, is necessary to maintain the predefined load.

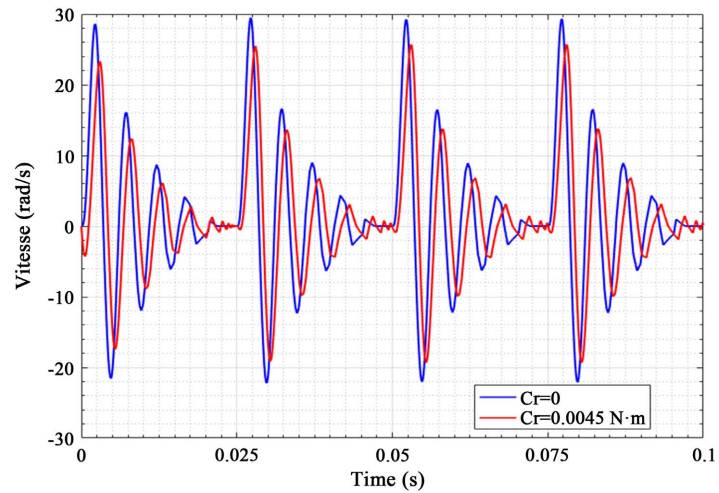


Figure 6. Evolution of rotation speeds.

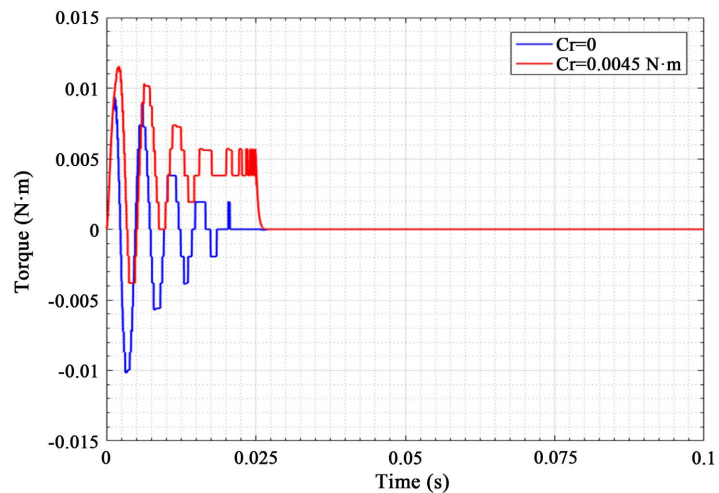


Figure 7. Evolution of electromagnetic torque.

Figure 8 illustrates the phase portraits, which depict the speed of rotation as a function of the displacement of the moving armature. This phase illustrates the periodicity of the rotor's movement around the stable equilibrium position without any hindrance. It is observed that under load, the oscillations persist around the equilibrium position, as evidenced by a strengthening of the line at the centres of the trajectories described by the rotor in **Figure 8**.

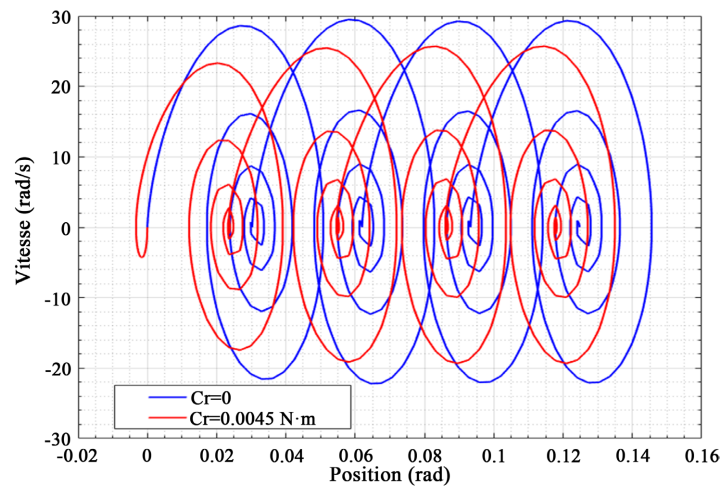


Figure 8. Phase portraits.

4. Conclusions and Outlook

This paper presents the dynamic performance of the HVRM with a stator magnet. The aforementioned performances are evaluated utilising data derived from the 3D finite element calculation integrated into the dynamic model. The combination of the aforementioned method of calculating dynamic performance with the finite element method yielded satisfactory results. The model accounts for the non-linearity and three-dimensional nature of the MRVH. The evaluation of this machine in this study is complete and accurate, as it incorporates the full range of relevant factors, including geometric complexity, winding end effects and permanent magnet configuration. The machine under investigation is capable of providing the torque required to hold a load of 0.0045 N·m. It may therefore be considered a potential candidate for use in a drive system with a load not exceeding the predicted value. Nevertheless, should the load be increased, the machine will become slower and may exhibit a different behaviour.

As a prospective outcome of this research, we intend to propose a methodology for the reduction of ripples in the characteristic quantities of an HVRM, conduct an experimental validation of the structure and perform a chaotic control of the dynamics of the MRVH in order to optimise the strange behaviour observed.

Conflicts of Interest

The authors declare no conflicts of interest regarding the publication of this paper.

References

- [1] Husain, I. and Ehsani, M. (1996) Torque Ripple Minimization in Switched Reluctance Motor Drives by PWM Current Control. *IEEE Transactions on Power Electronics*, **11**, 83-88. <https://doi.org/10.1109/63.484420>
- [2] Moulton, B. (1994) Conception et alimentation électronique des machines à réluctance variable à double saillance. Chez Technical Report, HDR, École Normale Supérieure.

- [3] Kada, B.N. (2015) Contribution à la modélisation par la méthode des réseaux des reluctance. Thèse de Doctorat, Université d'Oran Mohamed Boudiaf.
- [4] Idir, K., Chang, L. and Dai, H. (1998) Improved Neural Network Model for Induction Motor Design. *IEEE Transactions on Magnetism*, **34**, 2948-2951. <https://doi.org/10.1109/20.717688>
- [5] Fankem, E.D.K., Takorabet, N., Meibody-Tabar, F. and Michel Sargos, F. (2010) Non Linear Finite Element-Circuit Model of a Hybrid Stepping Motor. *COMPEL—The International Journal for Computation and Mathematics in Electrical and Electronic Engineering*, **29**, 957-963. <https://doi.org/10.1108/03321641011044370>
- [6] Guidkaya, G. (2018) Machine à réluctance variable: Approches par la commande et par la structure pour un fonctionnement pas à pas en hautes fréquences de commutation. Thèse de Doctorat, Université de Ngaoundéré.
- [7] Thamir, H.A. (2018) Various Control Strategies on Torque Ripple Minimization for Switched Reluctance Motor. *IOP Conference Series: Materials Science and Engineering*, **454**, Article ID: 012085. <https://doi.org/10.1088/1757-899X/454/1/012085>
- [8] Hilaire, B.D. (2019) Méthodes des éléments finis 3D et le couple de denture d'une machine à réluctance variable hybride. Editions Universitaires Européennes.
- [9] Faiz, J. and Finch, J.W. (1993) Aspects of Design Optimisation for Switched Reluctance Motors. *IEEE Transactions on Energy Conversion*, **8**, 704-713. <https://doi.org/10.1109/60.260984>
- [10] Lim, K.-C., Hong, J.-P. and Kim, G.-T. (2001) Characteristic Analysis of 5-Phase Hybrid Stepping Motor Considering the Saturation Effect. *IEEE Transactions on Magnetism*, **37**, 3518-3521. <https://doi.org/10.1109/20.952651>
- [11] Lawrenson, P.J., Stephenson, J.M., Fulton, N.N., Blenkinsop, P.T. and Corda, J. (1980) Variable-Speed Switched Reluctance Motors. *IEE Proceedings B Electric Power Applications*, **127**, 253-265. <https://doi.org/10.1049/ip-b.1980.0034>
- [12] Moallem, M. and Ong, C.-M. (1990) Predicting the Torque of a Switched Reluctance Machine from Its Finite Element Field Solution. *IEEE Transactions on Energy Conversion*, **5**, 733-739. <https://doi.org/10.1109/60.63147>
- [13] Sadowski, N. (1993) Modélisation des machines électriques à partir de la résolution des équations du champ en tenant compte du mouvement et du circuit d'alimentation (Logiciel EFCAD). Thèse de Doctorat, Toulouse INP.
- [14] Zhou, P., Gilmore, J., Badics, Z. and Cendes, Z.J. (1998) Finite Element Analysis of Induction Motors Based on Computing Detailed Equivalent Circuit Parameters. *IEEE Transactions on Magnetism*, **34**, 3499-3502. <https://doi.org/10.1109/20.717825>
- [15] Kavanagh, R., Murphy, J. and Egan, M. (1991) Torque Ripple Minimization in Switched Reluctance Drives Using Self-Learning Techniques. 1991 *International Conference on Industrial Electronics, Control and Instrumentation*, Kobe, 28 October-1 November 1991, 289-294. <https://doi.org/10.1109/IECON.1991.239292>
- [16] Redjem, R. (2010) Modélisation et optimisation d'une structure de machine à réluctance variable dédiée aux énergies renouvelables. Thèses de Doctorat, Université Mentouri de Constantine.
- [17] Belghith, S. (1997) Méthodes algébriques et numériques pour l'étude de comportements complexes de systèmes non linéaires. Thèse de Doctorat, Faculté des Sciences de Tunis.